Glutamate Receptor–Like Genes Form Ca^{2+} Channels in Pollen Tubes and Are Regulated by Pistil d-Serine

Erwan Michard *et al.*

Science **332**, 434 (2011);
DOI: 10.1126/science.1201101

Glutamate Receptor–Like Genes Form Ca^{2+} Channels in Pollen Tubes and Are Regulated by Pistil D-Serine

Erwan Michard,[1]* Pedro T. Lima,[1] Filipe Borges,[1] Ana Catarina Silva,[1] Maria Teresa Portes,[1] João E. Carvalho,[1] Matthew Gilliham,[2] Lai-Hua Liu,[3] Gerhard Obermeyer,[4] José A. Feijó[1,5]†

Elevations in cytosolic free calcium concentration ($[Ca^{2+}]_{cyt}$) constitute a fundamental signal transduction mechanism in eukaryotic cells, but the molecular identity of Ca^{2+} channels initiating this signal in plants is still under debate. Here, we show by pharmacology and loss-of-function mutants that in tobacco and *Arabidopsis*, glutamate receptor–like channels (*GLR*s) facilitate Ca^{2+} influx across the plasma membrane, modulate apical $[Ca^{2+}]_{cyt}$ gradient, and consequently affect pollen tube growth and morphogenesis. Additionally, wild-type pollen tubes grown in pistils of knock-out mutants for serine-racemase (*SR1*) displayed growth defects consistent with a decrease in GLR activity. Our findings reveal a novel plant signaling mechanism between male gametophyte and pistil tissue similar to amino acid–mediated communication commonly observed in animal nervous systems.

Pollen tubes are a model system for tip growth, a cellular growth mechanism common to fission yeast, filamentous fungi, neurons, and root hairs. Pollen tubes growing in vitro display regular oscillations in many parameters with the same period but often with different phase relationships (*1*). These include vesicle trafficking, cell wall precursor exocytosis, actin microfilament polymerization, apical ion flux, cytosolic pH, and cytosolic Ca^{2+} concentration ($[Ca^{2+}]_{cyt}$). The interaction of all these oscillating cellular processes integrate to produce oscillations in growth rate, which, in particular in vitro conditions, have been observed in most species so far analyzed (*1*, *2*). Currently, it is not obvious which of these cellular parameters take part in the control of oscillations or are outputs of a core pacemaker, and no physiological role for these oscillations has been proven (*2*, *3*). However, apical $[Ca^{2+}]_{cyt}$ gradients and oscillations, acting in concert with other transduction mechanisms, are widely accepted as a central regulatory mechanism of growth (*4*) and take part in downstream processing of external directional cues (*5*) like nitric oxide (*6*) or LUREs (*7*). Previously, Ca^{2+} channel activity in pollen has been proposed by electrophysiology [e.g., (*8*–*10*)] or by genetic analysis of cyclic nucleotide-gated channels (*11*). One Ca^{2+} channel expressed on the tonoplast (TPC1) (*12*) has been characterized at the molecular level, but so far the proof linking a specific gene to the respective plasma membrane Ca^{2+} channel activity has been resilient to most approaches in plant cells. In the present work, we investigate the role of plant homologs to the ionotropic glutamate receptor–like (GLR) family in the generation of $[Ca^{2+}]_{cyt}$ gradients and oscillations through apical Ca^{2+} influx and draw conclusions about the central role of these channels in pollen tube morphogenesis and guidance.

GLRs form Ca^{2+}-permeable channels that control pollen tube $[Ca^{2+}]_{cyt}$ and growth. Twenty ionotropic *GLR*s have been identified in the genome of *Arabidopsis*. Although definitive proof for the involvement of *GLR*s in Ca^{2+} channel activity across the plasma membrane is still missing (*13*), presence of plant *GLR*s has been correlated with increases in $[Ca^{2+}]_{cyt}$ (*14*–*17*), plasma membrane depolarization (*15*, *17*–*19*), and nonselective cation channel activity (*13*, *14*). Given that six GLRs are expressed in pollen (*20*), we tested the hypotheses that these genes could encode functional Ca^{2+} channels, as is the case in animals, and are involved in pollen tube growth. First, a pharmacological screen was conducted in the well-characterized tobacco pollen tube system (*4*), and the growth rate was monitored in the presence of GLR specific antagonists (DNQX 250 μM, CNQX 250 μM, and AP-5 50 μM, concentrations previously shown effective in plants) (*21*). All significantly inhibited tobacco pollen tube growth rate (AP-5 > CNQX > DNQX), suggesting a role for GLRs in pollen tube growth (fig. S1A). GLR agonistic amino acids were also screened for the same parameter (D-serine, L-serine, L-glutamate, and glycine) (*21*) (fig. S1B). Interestingly, L-Glu showed no effect, whereas Gly and D-Ser significantly increased growth rate (fig. S1B). However, Gly activated pollen tube growth over the whole concentration range, whereas D-Ser had a stronger stimulation and a concentration-dependent biphasic response (fig. S1B), as expected for a drug increasing $[Ca^{2+}]_{cyt}$ through Ca^{2+}-channel activation. For instance, in root hairs, another tip-growing system in which Ca^{2+} channel activity was measured (*22*), a threshold $[Ca^{2+}]_{cyt}$ is necessary for growth, but further increases in $[Ca^{2+}]_{cyt}$ inhibit growth (*23*). Additionally, D-Ser, but neither Gly nor any other amino acid tested, induced waving in pollen tubes morphology (fig. S1C), a process typically dependent on changes in $[Ca^{2+}]_{cyt}$ (*24*).

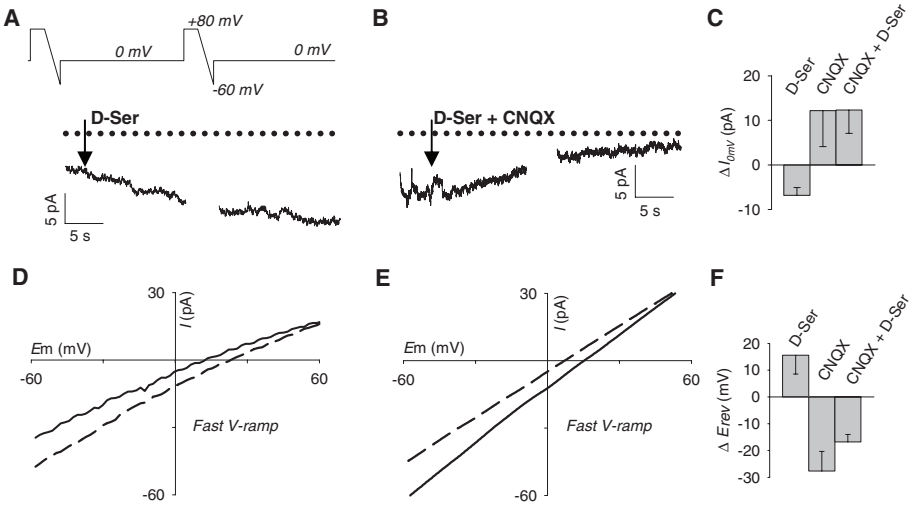

Fig. 1. Whole-cell Ca^{2+} currents in tobacco pollen tube tip protoplasts. (**A** and **B**) Effects of D-Ser (1 mM) ± CNQX (86 μM), respectively, on currents recorded at $V = 0$ mV. The V protocol is presented in (A) (same time scale as current traces). (**C**) Average current changes of experiments as presented in (A) and (B) ($n \geq 3$). (**D** and **E**) Fast voltage ramps (+80 to −60 mV) applied before (solid line) and after (dashed line) perfusion with D-Ser ± CNQX during the experiments presented in (A) and (B). +80 mV pulses preceded the voltage ramp. (**F**) Average E_{rev} shift induced by D-Ser, CNQX, and D-Ser + CNQX treatments ($n \geq 3$). Error bars indicate standard deviation.

[1]Instituto Gulbenkian de Ciência, Rua da Quinta Grande, 6, P-2780-156 Oeiras, Portugal. [2]Waite Research Institute and School of Agriculture, Food and Wine, University of Adelaide, PMB 1, Glen Osmond, SA 5064, Australia. [3]Key Laboratory of Plant and Soil Interaction, College of Resources and Environmental Sciences, China Agriculture University, 100193 Beijing, China. [4]Molecular Plant Biophysics and Biochemistry, Department of Molecular Biology, University of Salzburg, Billrothstrasse 11, 5020 Salzburg, Austria. [5]Universidade de Lisboa, Faculdade de Ciências, Departamento de Biologia Vegetal, Campo Grande C2, 1749-016 Lisboa, Portugal.

*Present address: Biochimie et Physiologie Moléculaire des Plantes, UMR 5004 CNRS-INRA-SupAgro-UM2, Campus INRA-Supagro, place Viala, 34060 Montpellier cedex 2, France.
†To whom correspondence should be addressed. E-mail: jfeijo@fc.ul.pt

The effects of D-Ser and CNQX on growth and tube morphogenesis were antagonistic, which suggests a common target for both agents (fig. S1, C to E). The crossed specificity of both these drugs strongly suggests that the only such target may be a member of the GLR family.

To test the hypothesis that GLR activity is involved in generating changes in $[Ca^{2+}]_{cyt}$, as suggested by the effect of D-Ser on pollen tube growth and morphogenesis, $[Ca^{2+}]_{cyt}$ was monitored using the ratiometric probe YC3.1-CaMeleon (*25*). The application of D-Ser increased $[Ca^{2+}]_{cyt}$, extended the gradient toward the subapical zone (fig. S2), and inhibited pollen tube growth. Given the positive correlation between growth rate and the $[Ca^{2+}]_{cyt}$ gradient (*26*), this result is suggestive of the opening of tip-localized plasma membrane Ca^{2+} channels by D-Ser.

To determine the action of GLR agonists and antagonists on plasma membrane transporters, whole-cell ion currents of protoplasts isolated from the apex of tobacco pollen tubes were measured using the patch-clamp technique (Fig. 1 and fig. S3). Protoplasts exhibited an instantaneous current on voltage steps from –80 to +80 mV (fig. S3A). When clamped at V = 0 mV, D-Ser induced an increase in negative current, whereas addition of the GLR antagonist CNQX reduced this current even in the presence of D-Ser (Fig. 1, A to C). Additionally, D-Ser induced a shift of the reversal potential (E_{rev}) to more positive voltage values (Fig. 1, D and F, and fig. S3, A and B). Chloride (Cl^-), protons (H^+/H_3O^+) and Ca^{2+} are the three permeable ions in the pipette and bath solutions. The positive shift in direction to the E_{rev} of Ca^{2+} and H^+ ($E_{Ca}{}^{2+}$ = 136 mV versus E_{Cl-} = 0 mV and E_{H+} = 111 mV) upon D-Ser application indicates an increase in H^+ (i.e., through H^+/amino acid cotransporter) or Ca^{2+} permeability. D-Ser (1 mM) does not affect significantly either H^+ fluxes (fig. S5) or intracellular pH (measured with the ratiometric pHluorin probe) (fig. S6) at the tube apex, discarding the hypothesis of an activation of an H^+ conductance by D-Ser at the plasma membrane. In accordance, application of CNQX (±D-Ser) and its opposite effect on E_{rev} implied a decrease in Ca^{2+} permeability (Fig. 1, E and F). These results are in accordance with a Ca^{2+}-permeable GLR channel in the plasma membrane of the pollen tube tip that is induced by D-Ser and blocked by CNQX.

GLR activity controls $[Ca^{2+}]_{cyt}$. The activity of plasma membrane Ca^{2+} channels should also be reflected as an inward flux of Ca^{2+} from the extracellular medium at the tip of the pollen tube, measurable with Ca^{2+}-specific vibrating microelectrodes (Fig. 2 and fig. S4). Both D-Ser (but not L-Ser) and Gly induced a reproducible increase in averaged Ca^{2+} influx (Fig. 2, A and D, and fig. S4, A to D and G), whereas antagonists CNQX, DNQX, and AP-5 had an inhibitory effect (Fig. 2, B to D, and fig. S4F). This D-Ser-induced effect was specific for Ca^{2+} fluxes, whereas only minor changes in H^+ fluxes and cytosolic pH could be detected (figs. S5 and S6), thus demonstrating that no amino acid/H^+ cotransport is induced by D-Ser. In addition to changes in Ca^{2+} flux intensity, D-Ser reproducibly triggered strong sustained oscillations (fig. S4C), especially notorious on non-oscillating tubes (usually ~30% of all measured tubes) (*25*). More generally, GLR agonists and antagonists respectively increased or decreased the oscillation amplitudes. To quantify this effect of GLR effectors on Ca^{2+} signature, we dissociated Ca^{2+} influx into two components for each time-lapse record: a basal, non-oscillating component defined by the minimum flux value from each cycle; and an oscillating component integrating all the fluxes above this base line. As shown in Fig. 2E, CNQX preferentially inhibited the oscillating component, whereas D-Ser increased the amplitude of the oscillations without significantly activating the non-oscillating fluxes.

***Atglr1.2* and *Atglr3.7* knock-out plants have male reproductive phenotypes.** To obtain further molecular evidence of a role of GLR activity in pollen tube growth and, importantly, for elucidation of the specific genes involved in generating the GLR properties in pollen tubes, the model plant *Arabidopsis* was used. Transferred DNA (T-DNA) insertion lines for the six GLRs expressed in *Arabidopsis* pollen grains (*20*) were harvested and their pollen germinated in vitro. Pollen tubes from *Atglr3.7-1* (At2g32400) and *Atglr1.2-1* (At5g48400) displayed distinct phenotypes: *Atglr3.7-1* tubes grew slower than wild type, and *Atglr1.2-1* tubes displayed abnormally deformed tips and tubes (Fig. 3 and figs. S8 and S9). *GLR1.2* and *GLR3.7* expression in pollen was confirmed by reverse transcriptase polymerase chain reaction (RT-PCR) using total RNA isolated from fluorescence-activated cell sorting–purified pollen grains (fig. 3A and fig. S9A). Both mutants also displayed a decreased number of seeds per silique, suggesting partial male sterility (Fig. 3B and fig. S9B). The growth rate decrease in the AtGLR3.7 mutant was further confirmed by crossing with wild-type/*quartet* mutant lines (fig. S9, C and D). *Atglr1.2* knock-out plant lines were particularly interesting because the phenotype mimicked the CNQX effect previously shown with in vitro–grown tobacco pollen tubes. Interestingly, also in *Arabidopsis*, CNQX-induced pollen tube deformations were characterized by regular enlargements of the tube, phenocopying the trait present in *Atglr1.2-1* pollen tubes (Fig. 3C). Abnormal pollen tubes were also visible in planta by callose staining using aniline blue on wild-type pistils pollinated with *Atglr1.2-1* pollen grains (fig. S8B). To investigate whether *GLR1.2* had a specific effect on the pollen tube physiology in the plant, we transformed *Arabidopsis* with a *GLR1.2* antisense complementary DNA (cDNA) under the control of the pollen-specific promoter LAT59. Pollen tubes from this plant line displayed similar tube deformation and decrease of seed set per silique to the *Atglr1.2-1* line, supporting a specific role of *GLR1.2* in the pollen tube growth (Fig. 3B). The transformed line also expressed the GFP (under the control of the pollen-specific LAT52 promoter), allowing a fast segregation analysis of plants obtained from a self-cross of heterozygous plants for the antisense construct. F1 plants scored 28.2% wild type, 53.1% heterozygous, and 18.7% homozygous for the antisense (n = 209) instead of the 25:50:25 expected if the construct had no effect on male fertility.

***GLR1.2* controls Ca^{2+} fluxes across the plasma membrane of *Arabidopsis* pollen tubes.** Because GLR activity was involved in Ca^{2+} influx generation in tobacco (Fig. 2), we measured apical Ca^{2+} fluxes in the *Atglr1.2-1* insertion line, too (Fig. 3D). In wild-type pollen tubes, Ca^{2+} fluxes oscillated in tubes longer than ~100 μm. We quantified changes

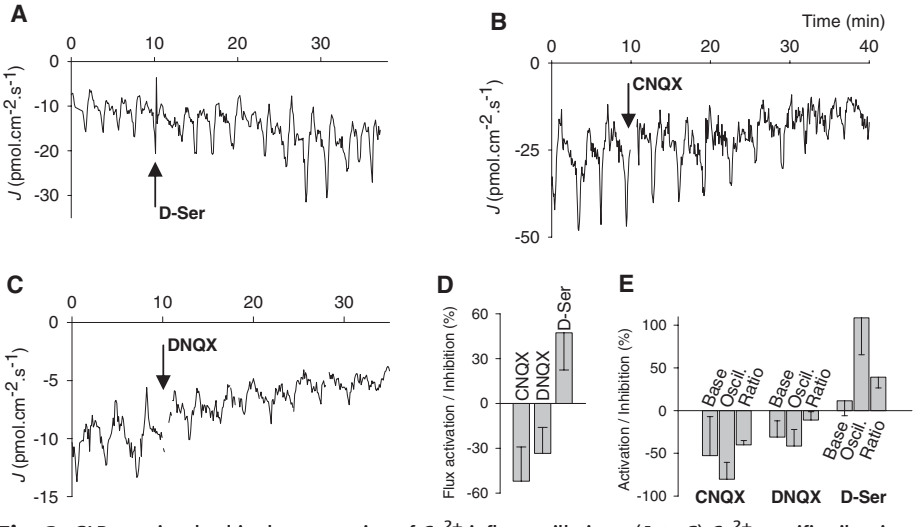

Fig. 2. GLRs are involved in the generation of Ca^{2+} influx oscillations. (**A** to **C**) Ca^{2+}-specific vibrating-probe measurements recorded at the tip of tobacco pollen tubes: D-Ser (1 mM), CNQX (250 μM), and DNQX (250 μM) (negative flux indicates Ca^{2+} movement into pollen tube). (**D**) Effect on average influx (compared to control) after application of CNQX (250 μM, n = 5), DNQX (250 μM, n = 6), and D-Ser (1 mM, n = 5) application. (**E**) Effect of DNQX, CNQX, and D-Ser, respectively on the non-oscillating flux component (base), oscillating flux component (oscil.), and flux ratio oscil./base. CNQX and D-Ser preferentially affect the oscillating component. Error bars indicate standard deviation.

in wave features of these oscillations as described previously for tobacco pollen tubes. Although no significant difference was recorded in average current intensity between wild-type and *glr1.2-1* pollen tubes, we detected a qualitative difference on the oscillatory behavior. Oscillating Ca^{2+} flux represented 59.7% ± 4.1 (n = 13) of total Ca^{2+} fluxes in wild type, but they represented only 33.2% ± 2.3 (n = 13) in pollen tubes from the *glr1.2-1* line (Fig. 3, D and F). This phenotype shows that, as in tobacco, *GLR*s are involved in the generation of Ca^{2+} influx oscillations in *Arabidopsis* pollen tubes. CNQX phenocopied this result, showing no significant difference in the average flux intensity but significant differences in the oscillation amplitude (Fig. 3, E and F). These results further confirm that GLR activity is involved in Ca^{2+} signaling in the pollen tube by controlling $[Ca^{2+}]_{cyt}$ through Ca^{2+} influxes. In particular, the effect of GLRs seems specific to the modulation of the oscillatory "Ca^{2+} signature," a hallmark of Ca^{2+} signaling in eukaryotic cells (*27*).

D-Ser plays an active role in pollen tube growth in vitro. Interestingly, the most active agonist of GLR activity in pollen tubes of tobacco and *Arabidopsis* was D-Ser. *GLR1.2* disruption had a similar effect as decreasing D-Ser–dependent GLR activity with CNQX. This result was unexpected because D-Ser is a very rare amino acid, although it is the subject of active research because of its role as a neuromodulator in specific neuronal circuits (*28*). The activity of a racemase is required to generate D-Ser from the physiologically inactive L-Ser. We thus investigated D-Ser formation and effects in *Arabidopsis*. As in tobacco, it increased $[Ca^{2+}]_{cyt}$ measured with the YC3.6 probe (Fig. 4) and increased Ca^{2+} influx and oscillation amplitudes at a physiological concentration (100 μM) (Fig. 5A). The induction of oscillations by D-Ser is particularly clear on $[Ca^{2+}]_{cyt}$ (Fig. 4D).

So far, only one gene has been identified in the *Arabidopsis* genome (*SR1* At4g11640) that corresponds to a serine-racemase activity in vitro (*29*). According to microarray data, this serine-racemase is expressed in the pistil, and particularly in the ovule (*30*). We cloned the serine-racemase gene promoter and performed a β-glucuronidase fusion assay on flowers harvested from transgenic plants expressing the construct. In three independent lines, β-glucuronidase was detected all over the pistil but, as confirmed by the microarray data, was particularly strong in the ovule, especially in the region close to the micropyle (inset, Fig. 5B). Immunolocalization of D-Ser in the pistil (Fig. 5C; D-Ser in blue, red is autofluorescence) confirmed the serine-racemase expression pattern. To demonstrate a correlation between the distribution of D-Ser and the expression of *SR1*, we characterized an insertion line for the serine-racemase gene (Fig. 5, D and E). A very weak D-Ser signal was detected in *sr1-1* pistils by immunolocalization (Fig. 5D), demonstrating that serine-racemase synthesizes D-Ser in plants. We further investigated whether the absence of normal levels of D-Ser could effect abnormal pollen tube growth in vivo. Pistils from the *sr1-1* line were thus pollinated with wild-type pollen grains, and pollen tubes were imaged by aniline blue staining (Fig. 5E). We systematically observed deformations and branching of wild-type tubes grown in pistils of the *sr1-1* genetic background. Remarkably, these deformations mimicked both the phenotype of *Atglr1.2-1* or CNQX-treated pollen tube grown in vitro and *Atglr1.2-1* pollen tube

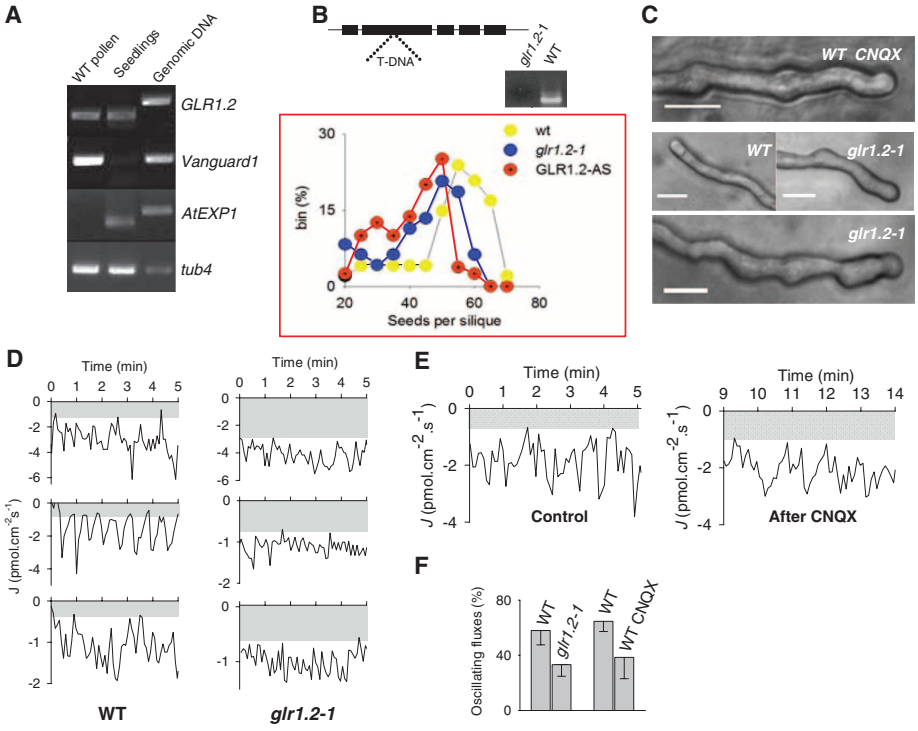

Fig. 3. *GLR1.2* is involved in *Arabidopsis* pollen tube morphogenesis and in Ca^{2+} apical influx oscillations. (**A**) RT-PCR analysis for *GLR1.2*, *Vanguard1* (At4g12730 pollen-specific) (*20*), *AtEXP1* (At2g47040 absent in pollen) (*20*), and *TUB4* expression in wild-type pollen (lane 1) and seedlings (lane 2). Lane 3 is PCR performed on genomic DNA (positive control). (**B**) *Atglr1.2-1* insertion line showing T-DNA located within the second exon. The transcript from *GLR1.2* was not detected by RT-PCR in inflorescence of *Atglr1.2-1* (inset). Number of seeds per silique in wild-type, *Atglr1.2-1* and *GLR1.2*-antisense plants (distribution curves, n > 100). (**C**) *Arabidopsis* wild-type pollen tube grown in the presence of CNQX (172 μM, upper panel) and *Atglr1.2-1* pollen tube grown in control condition (lower panel). (**D**) Typical Ca^{2+}-specific vibrating probe recordings in growing pollen tube of wild-type and *Atglr1.2-1*. (**E**) Effect of CNQX (172 μM) on Ca^{2+} apical influx in wild-type pollen tubes. (**F**) Ratio of oscillating Ca^{2+} flux in *Atglr1.2-1* compared with wild type in the presence of CNQX compared with control condition (wild-type plants).

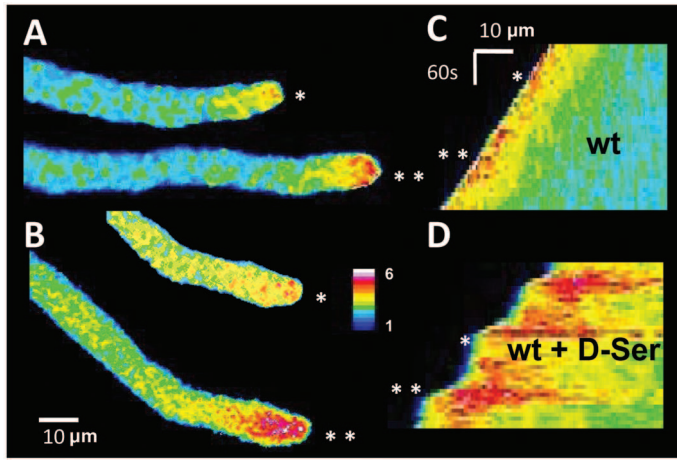

Fig. 4. D-serine increases $[Ca^{2+}]_{cyt}$ in *Arabidopsis* pollen tubes. (**A**) Typical YC3.6 cameleon imaging in a growing *Arabidopsis* pollen tube (n = 10). Upper and lower panels, respectively, depict the minimum (*) and maximum (**) $[Ca^{2+}]_{cyt}$ at the tip of the same cell. (**B**) After D-Ser (5 mM) application, tubes exhibit an increase in $[Ca^{2+}]_{cyt}$ (n = 7) and an extension of the gradient toward the subapical zone. (**C** and **D**) Kymographs from the tubes presented in (A) and (B), respectively. Each horizontal line of the kymograph illustrates the $[Ca^{2+}]_{cyt}$ values along a line traced in the middle of the tube at one time point. The slope of the kymograph represents the growth rate of the tube. Note the increase in $[Ca^{2+}]_{cyt}$ and activation of oscillations by addition of D-Ser. Color scale represents the fluorescence resonance energy transfer ratio (3 ≈ 100 nM and 6 ≈ 0.5 μM) (*3*).

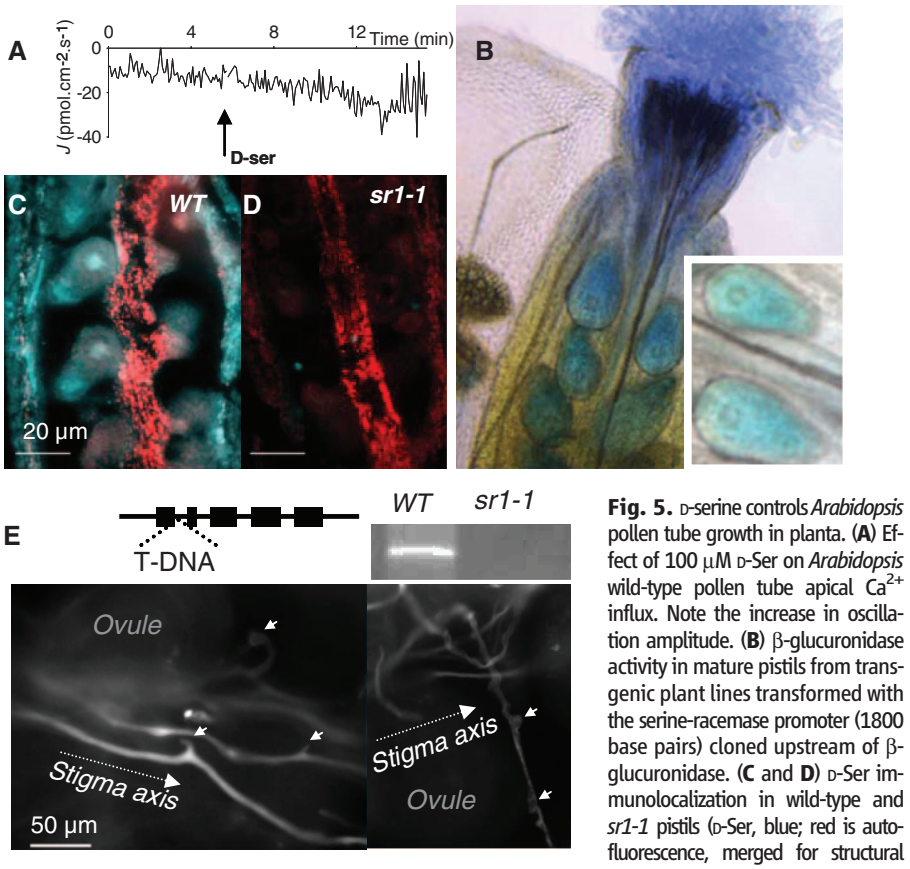

Fig. 5. D-serine controls *Arabidopsis* pollen tube growth in planta. (**A**) Effect of 100 µM D-Ser on *Arabidopsis* wild-type pollen tube apical Ca^{2+} influx. Note the increase in oscillation amplitude. (**B**) β-glucuronidase activity in mature pistils from transgenic plant lines transformed with the serine-racemase promoter (1800 base pairs) cloned upstream of β-glucuronidase. (**C** and **D**) D-Ser immunolocalization in wild-type and *sr1-1* pistils (D-Ser, blue; red is autofluorescence, merged for structural correlation). (**E**) Insertion line with a mutation for serine-racemase (*sr1-1*). No serine-racemase transcript was detected in insertion line. (Inset) RT-PCR on cDNA from flower. Images show callose staining on *sr1-1* pistils pollinated with wild-type pollen. Note balloon-like tip and branched pollen tubes, which are not observed in wild type.

grown in planta (Figs. 3C and 5D and fig. S8B). These results suggest that D-Ser formed in the pistil may have a subsidiary role in the navigation of pollen tubes by modulation of GLRs.

Discussion. Our results show that D-Ser activates GLRs in the apical region of pollen tubes, allowing Ca^{2+} permeation into the cytoplasm, thereby shaping the Ca^{2+} signature by modulation of both Ca^{2+} influx intensity and oscillation amplitudes. D-Ser concentration was measured in the µM range in plant extracts (*31*, *32*), and immunolocalization results show strong concentration differences in plant tissues, making it plausible that it may reach concentrations within the range we used in our in vitro experiments. However, we cannot overrule other effects of serine racemase, the latter having 20 times as much dehydratase activity as racemase activity (*29*). Animal GLRs play important roles in fast excitatory neurotransmission in the central nervous system. They are involved in neuron development as well as in neuron plasticity and participate in integrated cognitive processes such as memory and learning (*33*). The data we now report reveal conservation of an amino acid–based signal transduction involving oscillations, where similar channels perform their role by affecting specific kinetic properties of Ca^{2+}-induced neurotransmitter release. The previous demonstration of another amino acid (γ-aminobutyric acid)–ionotropic receptor (*34*) pair involved in pollen-pistil interaction makes an interesting parallel to the data we now present, suggestive of a much wider role of these kinds of mechanisms in cell-cell communication of plant tissue and organs.

Genes for putative cyclic nucleotide-gated channels were the first reported as plausible Ca^{2+} channels in pollen tubes (*11*). We attribute a physiological role to both *GLR* channels and Ca^{2+} oscillations in pollen tubes and make a direct link between these oscillations and pollen tube morphogenesis. Ca^{2+} oscillation properties directly participate in the coding of the Ca^{2+} signaling in the guard cell (*35*). Here, we prove that they are also important in the physiological function of pollen tubes and are not a mere by-product of signaling cascades controlling pollen tube growth and navigation in female tissues. Further molecular studies on plant *GLR*s in parallel with pollen tube growth modeling approaches may allow for deciphering the molecular mechanisms of generating and tuning Ca^{2+} oscillations in plant cells as well as the regulatory network linking oscillations and pollen tube morphogenesis.

References and Notes

1. N. Moreno, R. Colaço, J. A. Feijó, in S. Mancuso, Ed., *Rhythms in Plants: Phenomenology and Adaptive Significance* (Springer-Verlag, Berlin Heidelberg, 2007), pp. 39–62.
2. J. A. Feijó *et al.*, *Bioessays* **23**, 86 (2001).
3. M. Iwano *et al.*, *Plant Physiol.* **150**, 1322 (2009).
4. E. Michard, F. Alves, J. A. Feijó, *Int. J. Dev. Biol.* **53**, 1609 (2009).
5. J. A. Feijó, *J. Biol.* **9**, 18 (2010).
6. A. M. Prado, R. Colaço, N. Moreno, A. C. Silva, J. A. Feijó, *Molecular Plant* **1**, 703 (2008).
7. S. Okuda *et al.*, *Nature* **458**, 357 (2009).
8. H. Y. Qu, Z. L. Shang, S. L. Zhang, L. M. Liu, J. Y. Wu, *New Phytol.* **174**, 524 (2007).
9. Z. L. Shang *et al.*, *Plant Cell Physiol.* **46**, 598 (2005).
10. J. Wu *et al.*, *Plant J.* **63**, 1042 (2010).
11. S. Frietsch *et al.*, *Proc. Natl. Acad. Sci. U.S.A.* **104**, 14531 (2007).
12. E. Peiter *et al.*, *Nature* **434**, 404 (2005).
13. S. J. Roy *et al.*, *Plant Cell Environ.* **31**, 861 (2008).
14. V. Demidchik, P. A. Essah, M. Tester, *Planta* **219**, 167 (2004).
15. K. L. Dennison, E. P. Spalding, *Plant Physiol.* **124**, 1511 (2000).
16. C. Dubos, D. Huggins, G. H. Grant, M. R. Knight, M. M. Campbell, *Plant J.* **35**, 800 (2003).
17. O. Meyerhoff *et al.*, *Planta* **222**, 418 (2005).
18. Z. Qi, N. R. Stephens, E. P. Spalding, *Plant Physiol.* **142**, 963 (2006).
19. N. R. Stephens, Z. Qi, E. P. Spalding, *Plant Physiol.* **146**, 529 (2008).
20. C. Pina, F. Pinto, J. A. Feijó, J. D. Becker, *Plant Physiol.* **138**, 744 (2005).
21. R. Davenport, *Ann. Bot.* **90**, 549 (2002).
22. H. Miedema *et al.*, *New Phytol.* **179**, 378 (2008).
23. G. B. Monshausen, M. A. Messerli, S. Gilroy, *Plant Physiol.* **147**, 1690 (2008).
24. R. Malhó, N. D. Read, A. J. Trewavas, M. S. Pais, *Plant Cell* **7**, 1173 (1995).
25. E. Michard, P. Dias, J. A. Feijó, *Sex. Plant Reprod.* **21**, 169 (2008).
26. E. S. Pierson *et al.*, *Dev. Biol.* **174**, 160 (1996).
27. M. J. Berridge, *Biochim. Biophys. Acta* **1793**, 933 (2009).
28. H. Wolosker, E. Dumin, L. Balan, V. N. Foltyn, *FEBS J.* **275**, 3514 (2008).
29. Y. Fujitani *et al.*, *Phytochemistry* **67**, 668 (2006).
30. L. C. Boavida, F. S. Borges, J. D. Becker, J. A. Feijó, *Plant Physiol.* (2011).
31. T. Robinson, *Life Sci.* **19**, 1097 (1976).
32. H. Brückner, T. Westhauser, *Amino Acids* **24**, 43 (2003).
33. R. Dingledine, K. Borges, D. Bowie, S. F. Traynelis, *Pharmacol. Rev.* **51**, 7 (1999).
34. R. Palanivelu, L. Brass, A. F. Edlund, D. Preuss, *Cell* **114**, 47 (2003).
35. M. R. McAinsh, J. K. Pittman, *New Phytol.* **181**, 275 (2009).

Acknowledgments: E.M. acknowledges Fundação para a Ciência e a Tecnologia (SFRH/BPD 21056/2004), European Molecular Biology Organization (ASTF 193-2007), and Agropolis fellowships. We thank M. Watahiki (University of Hokkaido) for the YC3.1 construct and M. Iwano (Nara Institute of Science and Technology, Japan) for the YC3.6C *Arabidopsis* line. *glr1.2-1* and *glr3.7-1* insertion lines were originally characterized by P. Walch-Liu, X. Q. Qu, and Y. Y. Gong in L.-H.L.'s laboratory, in collaboration with M. Tester (University of Adelaide) and B. Forde (University of Lancaster). We thank N. Moreno and P. Almada for imaging support, A. Sommer for protoplast preparation, C. E. Tadokoro for immunofluorescence advice, J. Becker for helpful discussions on the genetic design of the experiments, P. Dias for help in oscillation analysis, and J. B. Thibaud (Institut National de la Recherche Agronomique-Supagro, Montpellier) for other institutional support to E.M. J.A.F.'s laboratory is supported by the Centro de Biologia do Desenvolvimento (FCT U664) and FCT grants BIA-BCM/108044/2008 and QUI/64339/2006. G.O.'s laboratory is supported by Austrian Science Fund grant P21298. L.-H.L. was supported by China National Science Foundation grant 30771288.

Supporting Online Material

www.sciencemag.org/cgi/content/full/science.1201101/DC1
Materials and Methods
Figs. S1 to S9
Table S1
References

1 December 2010; accepted 4 March 2011
Published online 17 March 2011;
10.1126/science.1201101